Published in final edited form as:
J Phys Chem B. 2010 April 8; 114(13): 4400–4406. doi:10.1021/jp9061412.

Distinguishing Polymorphs of the Semiconducting Pigment Copper Phthalocyanine by Solid-state NMR and Raman Spectroscopy

Medhat A. Shaibat[1], **Leah B. Casabianca**[1], **Diana Y. Siberio-Pérez**[2,#], **Adam J Matzger**[2,*], and **Yoshitaka Ishii**[1,*]

[1] Department of Chemistry, University of Illinois at Chicago, 845 West Taylor Street, Chicago IL 60607

[2] Department of Chemistry, University of Michigan, 930 N. University Ave., Ann Arbor, MI 48109

Abstract

Cu(II)(phthalocyanine) (CuPc) is broadly utilized as an archetypal molecular semiconductor and is the most widely used blue printing pigment. CuPc crystallizes in six different forms; the chemical and physical properties are substantially modulated by its molecular packing among these polymorphs. Despite the growing importance of this system, spectroscopic identification of different polymorphs for CuPc has posed difficulties. This study presents the first example of spectroscopic distinction of α- and β-forms of CuPc, the most widely used polymorphs, by solid-state NMR (SSNMR) and Raman spectroscopy. ^{13}C high-resolution SSNMR spectra of α- and β-CuPc using very-fast magic angle spinning (VFMAS) at 20 kHz show that hyperfine shifts sensitively reflect polymorphs of CuPc. The experimental results were confirmed by *ab initio* chemical shift calculations. ^{13}C and ^{1}H SSNMR relaxation times of α- and β-CuPc under VFMAS also showed marked differences, presumably because of the difference in electronic spin correlation times in the two forms. Raman spectroscopy also provided another reliable method of differentiation between the two polymorphs.

Introduction

Crystal polymorphism is a phenomenon observed for many organic molecules, and is defined as the ability of a compound to pack in more than one manner in the solid state, resulting in different interactions between the molecules in each crystal form, causing each polymorph to have different chemical, physical, and thermodynamic properties.

In the ink industry, the most widely used blue pigment is copper phthalocyanine (CuPc), or blue-15, with CuPc-based inks being used in gravure printing (food packages, greeting cards, magazines), paints, plastics and textiles.[1] This pigment has six different polymorphs, each with unique physical and chemical properties.[2] Because a pigment is, unlike dyes, highly insoluble in the delivery solvent, crystal form has a profound effect on end use. Thus, the preparation of pigment-based inks requires the production of pigment (nano)particles in specific crystal forms. In the case of CuPc-based inks, where the pigment can crystallize in six different forms that have diverse properties (ie. color tone, crystal morphology and size),

* To whom correspondence should be addressed. yishii@uic.edu; matzger@umich.edu.
# The current address: Empire State College, Three Washington Center, 2nd Floor, Newburgh, NY 12550

Supporting Information Available: ^{1}H inversion recovery SSNMR data, *ab initio* ^{13}C shift calculations, X-ray powder diffractions, and a peak table of FT-IR spectra for α- and β-CuPc are found as supporting information. This information is available free of charge via the Internet at http://pubs.acs.org.

[3] it becomes imperative to selectively crystallize one polymorph over others. More recently, CuPc has attracted renewed attention as an archetypal molecular semiconductor that forms a basis of organic optoelectronic devices such as organic solar cells[4,5] and organic transistors[6,7]; the crystal forms are likely to modulate the optical/electric properties of the devices.[8] Of the six crystal forms, the two most commercially important are the metastable α-form and the stable β-form, which are reddish-blue and greenish-blue respectively.[2] Only the X-ray crystal structure of β-CuPc is known.[9] The structure of α-CuPc has been predicted to be similar to that of α-PtPc due to the resemblance in the lattice constants of both unit cells.[10] A recent study of CuPc crystals grown on KCl by transmission electron diffraction, however, suggests that α-CuPc has a molecular packing pattern that differs from that of α-PtPc.[3] Despite the industrial applications and the growing scientific importance of CuPc in multiple forms, no previous spectroscopic studies have shown that distinctions of the polymorphs are possible. One approach to gain additional structural information for polymorphs unable to be coaxed into single crystal form is solid-state NMR (SSNMR) spectroscopy.[11-16] This has not been applied to CuPc primarily because of various technical difficulties associated with large paramagnetic spin interactions in high-resolution SSNMR applications using magic-angle spinning (MAS). Recently, Ishii's group and others established a very-fast MAS (VFMAS) approach to observe ^{13}C and ^{1}H high-resolution SSNMR spectra for paramagnetic systems.[17-23] Using this approach, we demonstrated the feasibility of distinguishing polymorphs for paramagnetic complexes from ^{13}C and ^{1}H chemical shifts for the first time.[18,24]

In this study, we applied the VFMAS approach to distinguish between the different polymorphs of paramagnetic CuPc, in particular the α- and β-forms, as notable examples. We demonstrate that chemical shifts and T_1 relaxation rates observed in ^{13}C and ^{1}H VFMAS SSNMR spectra are very sensitive probes of molecular packing for these systems. Comparison with Raman and infrared (IR) spectroscopy, which have been also widely used to distinguish among polymorphs, is also discussed. Our new Raman data suggest that notable differences are observed between the two crystal forms.

Results and Discussion

Figure 1 shows ^{13}C VFMAS SSNMR spectra of (a) α- and (b) β-CuPc with (c) the corresponding IR spectra (blue: α-form and red: β-form). For the α-CuPc (Fig. 1a), two resolved resonances were observed at 179 and 197 ppm. These signals were assigned to the two different CH groups (CH(1) and CH(2)) in phthalocyanine based on the CH dipolar dephasing and dipolar INEPT experiments, as will be discussed below. In this sample, only CH and non-protonated carbons exist in the phthalocyanine ligand as shown in Fig. 1d. In Fig. 1a, the two strong peaks were observed. In contrast, Fig. 1b for the β-form shows only one strong peak at 180 ppm and one weaker yet resolved peak at 132 ppm. As will be discussed below, these signals were also assigned to the CH group(s). The diamagnetic shifts for the CH groups in the aromatic ring of the phthalocyanine without paramagnetic metals are approximately 120-150 ppm.[25] The ^{13}C isotropic chemical shift for paramagnetic compounds is generally divided into two components: hyperfine shift and diamagnetic shift. The former is mainly accounted for by the contact shift due to an unpaired electron in a paramagnetic metal ion, while the latter is well approximated by the chemical shift for a diamagnetic analog which does not have unpaired electron spin.[20,26] Although shifts due to electron spin-nuclear spin dipolar interactions (pseudo-contact shifts) also yield considerable *anisotropic* hyperfine shifts, the isotropic hyperfine shift due to this interaction is often negligible for Cu(II) compounds, for which the g-anisotropy is generally small.[20,27,28] The results above suggest that ^{13}C shifts are subject to relatively large hyperfine shifts due to paramagnetic Cu(II), which sensitively reflect the molecular packing or crystal form of the compound.[18,24] Unlike X-ray powder diffraction, NMR chemical shifts primarily depend on

local electronic environments. Thus, dramatically different hyperfine ^{13}C shifts observed for α- and β-CuPc clearly reflect significant difference in the electronic environments of the two compounds due to different molecular packing.

Infrared (IR) spectroscopy is another popular spectroscopic technique that is often used to distinguish between polymorphs. However, as shown in Fig. 1c, the IR spectra for the two forms show nearly identical spectral features, which make it very difficult to distinguish between these two forms. The results clearly demonstrate that ^{13}C SSNMR spectroscopy using VFMAS permits us to distinguish the two polymorphs, which were not distinguishable by IR spectroscopy and other spectroscopic methods. Despite the relatively small sample quantity (10-20 mg), the SSNMR spectra show reasonable S/N ratios in a range of hours without any isotope labeling. Raman spectra previously obtained for the α-form of CuPc[29] and for the β-form[30] did not indicate that distinction is possible. However, as will be discussed later, newly obtained Raman spectra of the two forms with superior resolution allow for differentiation between the two forms.

The line widths in the SSNMR spectra in Fig. 1 show considerable variations. For example, the line width for the peak at 179 ppm in the α-form in Fig. 1a is 2,230 Hz, while that for the peak at 197 ppm is 1,650 Hz. On the other hand, the width for the peak at 180ppm for the β-form in Fig. 1b is 3,370 Hz, while the peak at 132 ppm has a line width of 1,540 Hz. The fitting of each experimental spectrum with two primary Lorentzian components was performed with a line shape fitting function in Varian Spinsight software. Assuming that the electron spin localizes at a paramagnetic metal center and relaxation is through the Solomon relaxation mechanism via electron-nuclear dipolar relaxation, the paramagnetic T_2 relaxation time in solids is generally given by kR^6,[31,32] where R denotes the distance between the paramagnetic metal center to ^{13}C and k is a constant that depends of electron spin relaxation time of the metal center.[26] Thus, ^{13}C closer to the metal center tends to have a broader line (i.e. homogeneous line width $\propto 1/T_2$). Although considerable variations in T_2 relaxation properties and line widths are expected for this system, it is difficult to separate the line width due to paramagnetic T_2 relaxation from that due to inhomogeneous broadening such as ^{13}C shift distribution or non-paramagnetic T_2 relaxation due to insufficient decoupling.

To clarify the difference in the relaxation properties of these two forms, we performed ^{13}C T_1 experiments and analyzed the T_1 values of these two forms, as summarized in Table 1. ^{13}C T_1 can be used to elucidate structural information or signal assignments because ^{13}C T_1 value is also proportional to R^6.[20,26,28] For the α-form, we found that the peak at 179 ppm has a ^{13}C T_1 value of 38.3 ± 2.1 ms and the peak at 197 ppm has a ^{13}C T_1 of 25.1 ± 2.1 ms. The short relaxation times compared with ^{13}C T_1 in diamagnetic systems (in the order of 0.1-1 s) confirm that these signals are attributed to paramagnetic systems. The R^6 dependence suggests that for the ^{13}C species at 179 ppm, the ^{13}C-Cu(II) distance is, on average, about 1.07 fold longer (i,e. $(38.3/25.1)^{1/6}$) than that for ^{13}C at 197 ppm on the assumption that the paramagnetic electron spin is localized at Cu. The results suggest that the range of the ^{13}C-Cu(II) distances are similar for the two peaks. Although a deviation due to electron delocalization is expected, the factor (1.07) agrees reasonably well with the ratio of 1.19 (6.60/5.56) that was calculated from the Cu-CH distances for CH(1) (5.56 Å) and CH(2) (6.60 Å) in the α-form.[3] Based on an assumption that all CH(1) and CH(2) groups are in chemically very similar environments, we first interpreted that CH(1) and CH(2) may be assigned to the peaks at 197 ppm and 179 ppm, respectively. However, as will be shown by our *ab initio* chemical shift calculations, it is possible that all the CH(1) and CH(2) groups in CuPc are in different environments, yielding several NMR signals, a superposition of which appear to be the two peaks.

For the β-form, the peak at 180 ppm has a shorter ^{13}C T_1 of 8.6 ± 0.4 ms while the peak at 132 ppm has a ^{13}C T_1 of 14.0 ± 2.3 ms. Again, the short ^{13}C T_1 confirms that the sample is a paramagnetic species. These values indicate that the ratio of the ^{13}C-Cu(II) distances for ^{13}C at 177 ppm and 132 ppm is 1.08. This is also consistent with the distances of 5.51 Å and 6.55 Å for the CH(1) and CH(2) in the β-form (a ratio of 1.19).[9] For some of the CH(2) groups in the β-form, intermolecular Cu(II)-CH(2) distances are shorter (~5.5 Å); the T_1 values of such CH(2) groups may be reduced to a level comparable to that of CH(1) by the additional relaxation source. More importantly, the results show that the β-form has shorter ^{13}C T_1 values (8-14 ms) than those for the α-form (25-38 ms). Thus, the two forms are distinguishable based on ^{13}C T_1. The variation in ^{13}C T_1 presumably reflects different electron spin relaxation times, which are sensitive to inter-molecule Cu(II) distances and super exchange interactions between electron spins, both of which depend on the molecular packing.[28] The shorter ^{13}C T_1 values in the β-form indicate that this form is packed in a substantially different way, compared to the α-form.

Short ^{13}C T_1 values for these CH groups in the two polymorphs indicate that the non-protonated carbons (C_1, C_2), which are closer to Cu(II) and not observed in Fig. 1(a, b), are likely to have even shorter ^{13}C T_1 (~4 ms or less) and broader lines than those for the CH groups. It is noteworthy that for the systems that have conjugated π-electrons, the electron delocalization may not be a negligible factor in calculating averaged $<1/R^6>$, especially for ^{13}C closer to the metal centers. It is possible that the signals for non protonated carbons are quenched by very fast paramagnetic T_2 relaxation due to the electron delocalization. In our previous study of Fe(III) hemin,[28] which also has conjugated π-electron systems, it was difficult to observe ^{13}C in the ring of the heme groups. Although further studies are needed, it is most likely that the signals for the non-protonated ^{13}C are substantially broadened.

The signal assignments of ^{13}C VFMAS spectra shown in Fig. 1(a, b) are based on the ^{13}C-^{1}H dipolar dephasing experiments using the ^{13}C-^{1}H REDOR sequence, which was successfully applied for signal assignments of paramagnetic samples previously.[17,19] This experiment is designed to remove signals of protonated ^{13}C selectively. In the experimental condition utilized here (adopted from ref. [17]), this sequence removes most of the signals (~90%) for ^{13}CH and $^{13}CH_2$ for rigid systems while it removes only about 50% of $^{13}CH_3$ due to methyl rotation; about 80-90% signal should be retained for non-protonated ^{13}C.[17,19] Because there are no CH_3 or CH_2 groups in CuPc, the assignment of the peaks is relatively straightforward. In Fig. 2, the intensities without (top) and with (bottom) ^{13}C-^{1}H dipolar dephasing are compared for (a) α- and (b) β-CuPc. For the peak at 197 ppm in (a), about 94 ± 3 % of the signal was dephased, where the error was estimated from the noise level; this indicates that this ^{13}C is directly bonded to a proton. Likewise, for the peak at 179 ppm in (a), 91 ± 2 % of the signal was dephased. For the β-form in (b), the peaks at 180 ppm and 132 ppm were dephased by 91 ± 3% and 71 ± 13%, respectively. These results suggest that all these peaks in the two forms are attributed to ^{13}CH species rather than non-protonated ^{13}C. Therefore, these CH groups in the two forms are in very distinctive electronic environments reflected in the notably different hyperfine shifts.

To confirm the suggested assignments, we performed *ab initio* chemical shift calculations of ^{13}C chemical shifts. Tables 2 and 3 show the calculated diamagnetic shieldings, diamagnetic chemical shifts (δ_d), hyperfine shifts (δ_H) and expected chemical shifts ($\delta_d + \delta_H$) for carbons in α-CuPc (Table 2) and β-CuPc (Table 3). The atom numbering is shown in Fig. 1d. Figure 3 shows simulated spectra of ^{13}CH groups for (a) α-CuPc and (b) β-CuPc that were produced from the calculated ^{13}C shifts (blue) without broadening and (red) with Gaussian broadening. Although the effects of the neighboring molecules are generally not negligible,[24] these effects are not directly included in the present calculations because of the long computation time required by the relatively large size of the molecule. Yet, the

coordinates of the monomeric α- and β-CuPc reflect structural differences between the two forms. The simulated spectra reasonably reproduced the experimental spectra and present the different spectral features observed for α-CuPc and β-CuPc. Thus, the *ab initio* chemical shift calculations clearly demonstrate that the observed spectra are attributed to ^{13}CH groups. Therefore, despite the noticeable difference between experimental and calculated shifts for β-CuPc, the chemical shift calculations for the monomeric paramagnetic compounds provide useful guidance in evaluation and assignments of the experimental shifts.[24,33]

As found in Tables 2 and 3, the calculated chemical shifts for *non-protonated* ^{13}C (not shown in Fig. 3) exhibited much larger shifts in a range of 660-900 ppm and 650-850 ppm for the α- and β-forms, respectively. Large hyperfine shifts indicate a large imbalance between α- and β-spin density at that nucleus. As discussed above, these non-protonated ^{13}C groups are likely to have considerably shorter T_2 values than those for CH groups due to their vicinity to the paramagnetic metal center. The calculations also confirm that the CH carbons are experiencing hyperfine shifts. The expected diamagnetic shifts for all of these carbons (the shift in the absence of a paramagnetic center) are in a range of 120-130 ppm. However, the presence of contact hyperfine shifts leads to calculated shifts in the region of 165-190 ppm for α-CuPc, and 147-200 ppm for the β-form. We initially assumed that all the eight CH(1) and CH(2) carbons in a molecule are each in very similar chemical environments. The calculation results in Tables 2 and 3 suggest that this may not be entirely correct. As shown in Table 2 for the α-form, ^{13}CH(1) display a distribution of ^{13}C shifts in a range of 164-187 ppm while ^{13}CH(2) also showed a distribution in the similar range of 164-188 ppm. This result indicates that each of the peaks at 179 and 197 ppm in Fig. 1a may be comprised of a superposition of several signals of ^{13}CH(1) and ^{13}CH(2) as shown in Fig. 3a. A similar trend was found in calculated shifts for the β-form in Table 3. Despite the considerable heterogeneity predicted here, the expected peak positions for the CH groups reproduce well spectral positions observed in the experimental spectra. Since chemical shifts are sensitive to electronic structures, the present results suggest that electronic structures of α- and β-CuPc are reasonably well reproduced by calculations for isolated molecules. Further experiments and more elaborate calculation studies are needed for more accurate comparison between experimental and calculated shifts.

Next, we compared ^{1}H SSNMR spectra in Fig. 4. The spectrum for the α-form in Fig. 4a shows one main peak at 7.9 ppm. The spectrum for the β-form in Fig. 4b shows the main peak at a similar position (at 8.2 ppm). For the diamagnetic analogs ZnPc[34] and MgPc[35], the ^{1}H chemical shifts are reported to be in a range of 5-8 ppm and 5.9-7.0 ppm, respectively.

To confirm that these ^{1}H lines are correlated with the paramagnetically influenced ^{13}C shifts observed in Fig. 1, we collected a 2D ^{13}C/^{1}H correlation SSNMR spectrum of (a) α-CuPc and (b) β-CuPc under VFMAS in Fig. 5. 2D ^{13}C/^{1}H correlation NMR has been widely used to determine assignments and connectivity in organic molecules.[36] However, for paramagnetic systems, this technique has not been demonstrated because of the lack of effective polarization transfer techniques until recently. Our group earlier demonstrated the effectiveness of the dipolar INEPT sequence to obtain signal assignment and structural information for paramagnetic complexes.[19,20] Figure 5a shows ^{13}C /^{1}H correlation spectra of α-CuPc obtained with dipolar INEPT at τ = 5.0 μs. The major cross peaks at (ω_H, ω_C) = (7.9 ppm, 198 ppm) and (10.8 ppm, 178 ppm) show connectivities from the ^{1}H spins at 8.1 ppm and 10.5 ppm to the ^{13}C spins at ~200 and ~180 ppm, respectively. This indicates that these two carbon spins that exhibit hyperfine shifts are directly bonded to protons in the α-CuPc, which appear to show relatively small hyperfine shifts. Although there might be more

than the two peaks, it is difficult to resolve other peaks clearly because of the limited resolution. In Fig. 5b for β-CuPc, there are two major cross-peaks at (ω_H, ω_C) = (10.3 ppm, 178 ppm) and (5.4 ppm, 130 ppm), which again show that ^{1}H species connected to ^{13}C corresponding to the peaks at ~180 ppm and ~130 ppm have different electronic environments. Clearly, the 2D spectra for α- and β-CuPc allow us to distinguish the two forms of CuPc with confidence.

Although the ^{1}H chemical shifts for both forms of CuPc are similar to the shifts of the diamagnetic organic molecules, the ^{1}H T_1 values were found to be much shorter. For rigid diamagnetic organic molecules, ^{1}H T_1 values are typically of the orders of ca.1-10 s. We found that the ^{1}H T_1 values of the two forms are as distinctive as ^{13}C T_1 values. ^{1}H T_1 for the main peak at 7.9 ppm for the α-form is 5.6 ± 0.1 ms (R =0.978), while it is 1.4 ± 0.1 ms (R=0.967) for ^{1}H at 8.2 ppm in the β-form (see Fig. S2 and S3 in Supporting Information (SI)), where the standard deviation of the ^{1}H T_1 values in three separate trials were less than 0.1 ms for the two samples. Thus, one can clearly distinguish between the two polymorphs based on ^{1}H T_1 values.

Raman spectroscopy results

The vibrational frequencies of several phthalocyanine complexes have been previously reported,[37-39] including those of α- and β-CuPc.[29,30] While it has been shown that differences exist between Raman spectra of different H_2Pc polymorphs,[37] the comparison of spectra for four polymorphs of CuPc led others to conclude that no sufficiently distinct shifts could be observed between crystal forms.[39]

With the encouraging SSNMR data, we revisited the problem of distinguishing α-and β-forms of CuPc by Raman spectroscopy, as shown in Fig. 6. New Raman data collected for both α- and β-CuPc indeed prove that appreciable differences in the vibrational modes of both polymorphs do exist. These shift differences ($\Delta\nu$) were observed for five Raman bands, as detailed in Table 4. The largest difference was observed for the ν_{52} vibration, which is the result of the Cu—N deformation, and had a $\Delta\nu$ of 4.07 cm^{-1}. The next largest $\Delta\nu$'s belong to the ν_{14} and the ν_{28} modes, having magnitudes of 2.19 and 1.91 cm^{-1}. These bands have been assigned to the C-H bending of the benzene ring and the stretching of the macroring, respectively. The ν_{25} and the ν_{31} vibrations experienced the smallest shift differences. Although there are conflicting assignments for these bands,[30,38,40] all references agree that these arise due to deformations in the isoindole fragments of the CuPc structure.

Conclusion

The newly collected ^{13}C and ^{1}H SSNMR data using the VFMAS method provided a basis that α- and β-CuPc, which are widely used as organic semiconductors and pigments, are distinguishable by chemical shifts and relaxation properties from SSNMR analysis. Our study also showed that ^{13}C chemical sifts calculated by *ab initio* methods well reproduce experimental shifts, suggesting that electronic structures obtained by the calculations are likely to be correct. Newly performed Raman spectroscopy for the two forms also showed promising results for the two forms. It is likely that these two spectroscopic methods provide useful insights into analyzing structures of CuPc and other organic semiconductors in different polymorphs, which have long posed challenges in spectroscopic characterization.

Materials and Methods

Solid-state NMR Experiments

All the ^{13}C MAS experiments were recorded at 9.4 T with a Varian InfinityPlus 400 NMR spectrometer using a 2.5-mm home-built double/triple-resonance NMR magic-angle-spinning (MAS) probe. Samples of standard powder α- and β-CuPc were used as provided by Flint Ink. The X-ray powder diffraction (XRPD) patterns for these samples (Fig. S1 in SI) reproduced those previously reported for the two polymorphs.[41] The sample was packed as received in a 2.5-mm zirconia MAS rotor without further treatments. All the data were acquired at a spinning speed of 20,000 ± 5 Hz or 22,989 ± 5 Hz with a rotor-synchronous echo sequence. A π-pulse was applied at the end of the first rotor period after the initial magnetization was prepared by a π/2-pulse. Because paramagnetic isotropic shifts have a 1/*T*-dependence (Curie's law) in the high temperature approximation, both spinning speed and RF duty factor were found to affect observed chemical shifts. For experimental simplicity, unless otherwise mentioned, we indicated the temperature of VT cooling air (−10 °C) rather than that of a sample, which was about $0.0607(\nu_R)^2$ higher than that of the cooling air based on the $^{13}CH_3$ shift of $Cu(DL\text{-}Ala)_2$,[20] where ν_R denotes a spinning speed in kHz. The experimental ^{13}C chemical shifts were referenced to TMS at 0 ppm using the secondary external standard of ^{13}CH in adamantane at 38.56 ppm. ^1H chemical shifts were also referenced to TMS using the secondary external standard of H_2O at 4.7 ppm.

All the ^{13}C and ^1H MAS spectra were recorded with a rotor-synchronous echo sequence. For the SSNMR data in Fig. 1 and 2, the signals were acquired with 10 μs sampling intervals from the end of the second rotor cycles after the initial π/2-pulse. The ^{13}C pulse widths for π/2- and π-pulses were 2.5 and 5.0 μs, respectively. Signals were recorded during the acquisition periods of 10.3 ms for CuPc in Fig. 1(a, b) and Fig. 2(a, b). For the SSNMR experiments in Fig. 1 and 2, we used a background suppression scheme by Chen and Schmidt-Rohr.[42] For background suppression, a background spectrum was collected using the same pulse sequence but with the initial excitation by a π-pulse in place of a π/2-pulse. In this spectrum, signals for CuPc were negligible (not excited by a π-pulse) and only signals for the background ^{13}C that was remotely located from the sample coil were observed. The background spectrum was multiplied by 0.5,[42] and subtracted from the spectrum collected using a π/2-pulse. For the experiments in Fig. 2, we used ^{13}C-^1H REDOR experiments previously discussed.[17],[19] These RF pulses sufficiently cover the spectral widths of ~1000 ppm (±50 kHz).

For the ^1H spectrum in Fig. 4(a,b), the signals were acquired with 2 μs sampling intervals from the end of the second rotor cycle after the initial π/2-pulse. The recycle delay was 100 ms for the two spectra.

For Fig. 5, a pulse sequence for 2D $^{13}C/^1H$ correlation experiment with dipolar INEPT transfer was adopted from ref. [19]. A period of $\tau = 5.0$ μs was optimized for efficinent polarization transfer for CH groups. For both ^{13}C and ^1H spins, pulse widths for π/2- and π-pulses were 2.5 and 5.0 μs, respectively.

Ab initio Chemical Shift Calculations

Chemical shifts were calculated for the protons and carbons in a monomer of α- and β-CuPc based on the structures obtained by transmission electron diffraction[3] and X-ray crystallography,[9] respectively. Chemical shift calculations and carbon chemical shift referencing were done as described previously.[24] The positions of hydrogen atoms were optimized using the B3LYP/6-31G* level of theory while the positions of the heavy atoms were held fixed. Diamagnetic chemical shifts were calculated using a Zn analog of α- or β-CuPc using GIAO with B3LYP/6-311G. Fermi contact spin densities were similarly

calculated for the Cu species using UB3YP/6-311G. These were converted to hyperfine shifts using equations (3) through (5) in ref. [43] with $S = 1/2$ and $T = 298$K. Oldfield and coworkers have shown that the calculated ^{13}C shifts for Cu(II)(DL-alanine)$_2$ agree well with the experimental SSNMR shifts within the rms difference of 6.3 % with respect to the total spectral range.[33] Although the effects of Cu(II) in neighboring molecules are not included in the present calculations, our previous study for α- and β-Cu(II)(8-quinolinol)$_2$ showed that chemical shift calculations for monomeric forms reproduced ^{13}C hyperfine shifts reasonably well when inter-molecular Cu(II)-^{13}C distances are relatively long.[24] For a CuPc compound, a relatively small g-anisotropy ($|(g_{xx}-g_{zz})/g_{zz}|=0.05$) was reported by a previous EPR study; [44] the isotropic shift predicted from the pseudo contact shifts are small (at most 3 ppm) for the CH groups. Thus, the effects of pseudo contact shifts were neglected in the calculations.

Characterization of α- and β-CuPc by FTIR

The sample amount was ~1.1 mg for each, and the sample was then ground and mixed with ~ 170 mg of KBr. About 30 mg of the mixture was used to obtain a KBr pellet for the measurements . Measurements were obtained at room temperature with 256 scans. As listed in Table S1 in SI, the peak positions for all the major peaks are identical within the range of the error.

Raman Spectroscopy of α- and β-CuPc

Raman spectra were collected using a Renishaw inVia Raman Microscopy system equipped with a 50 mW 633 nm He-Ne laser, an 1800 lines/mm grating and a 20× SLMPlan objective (0.35 numerical aperture). During collection the slit width was kept at 50 μm while the laser power was kept at 1% to prevent sample heating. The scanning range was between 200 and 3200 cm^{-1}. For assignment of peak positions, the peak-fitting feature of ACD/Spec Manager UVIR software (ACD/Labs) was employed, using a Gaussian-Lorentzian function with a width limit of 15 cm^{-1}.

Supplementary Material

Refer to Web version on PubMed Central for supplementary material.

Acknowledgments

This work was supported primarily by the NSF CAREER program (CHE 449952) and also in part by Alzheimer's Association IIRG grant (08-91256), the Dreyfus Foundation Teacher-Scholar Award program, Flint Group Pigments, and the NIH RO1 program (AG028490). We thank Dr. InHwan Oh for valuable discussions.

References

1. Lobbert, G. Ullmann's Encyclopedia of Industrial Chemistry. 6th ed.. Wiley-VCH Verlag, GmbH; Weinheim: 2000.
2. Bernstein, J. Polymorphism in Molecular Crystals. Clarendon Press; Oxford: 2002.
3. Hoshino A, Takenaka Y, Miyaji H. Acta Crystallogr. B. 2003; 59:393. [PubMed: 12761409]
4. Yang F, Shtein M, Forrest SR. Nat. Mater. 2005; 4:37.
5. Yang F, Forrest SR. Adv. Mater. 2006; 18:2018.
6. Tang QX, Li HX, Liu YL, Hu WP. J. Am. Chem. Soc. 2006; 128:14634. [PubMed: 17090049]
7. Tang QX, Tong YH, Li HX, Ji ZY, Li LQ, Hu WP, Liu YQ, Zhu DB. Adv. Mater. 2008; 20:1511.
8. Bredas JL, Calbert JP, da Silva DA, Cornil J. Proc. Natl. Acad. Sci. U. S. A. 2002; 99:5804. [PubMed: 11972059]
9. Brown CJ. J. Chem. Soc. A. 1968:2488.
10. Brown CJ. J. Chem. Soc. A. 1968:2494.

11. Harris RK. Analyst. 2006; 131:351. [PubMed: 16496044]
12. Apperley DC, Fletton RA, Harris RK, Lancaster RW, Tavener S, Threlfall TL. J. Pharm. Sci. 1999; 88:1275. [PubMed: 10585222]
13. Schmidt A, Kababya S, Appel M, Khatib S, Botoshansky M, Eichen Y. J. Am. Chem. Soc. 1999; 121:11291.
14. Middleton DA, Le Duff CS, Peng X, Reid DG, Saunders D. J. Am. Chem. Soc. 2000; 122:1161.
15. Willans MJ, Wasylishen RE, McDonald R. Inorg. Chem. 2009; 48:4342. [PubMed: 19425611]
16. Hamaed H, Pawlowski JM, Cooper BFT, Fu RQ, Eichhorn SH, Schurko RW. J. Am. Chem. Soc. 2008; 130:11056. [PubMed: 18656917]
17. Ishii Y, Chimon S, Wickramasinghe NP. J. Am. Chem. Soc. 2003; 125:3438. [PubMed: 12643699]
18. Wickramasinghe NP, Shaibat M, Ishii Y. J. Am. Chem. Soc. 2005; 127:5796. [PubMed: 15839671]
19. Wickramasinghe NP, Ishii Y. J. Magn. Reson. 2006; 181:233. [PubMed: 16750405]
20. Wickramasinghe NP, Shaibat M, Casabianca LB, de Dios AC, Harwood JS, Ishii Y. J. Chem. Phys. 2008; 128:52210.
21. Kervern G, Pintacuda G, Zhang Y, Oldfield E, Roukoss C, Kuntz E, Herdtweck E, Basset JM, Cadars S, Lesage A, Coperet C, Emsley L. J. Am. Chem. Soc. 2006; 128:13545. [PubMed: 17031968]
22. Ouyang L, Aguiar PM, Batchelor RJ, Kroeker S, Leznoff DB. Chem. Commun. 2006:744.
23. Willans MJ, Sears DN, Wasylishen RE. J. Magn. Reson. 2008; 191:31. [PubMed: 18086543]
24. Shaibat MA, Casabianca LB, Wickramasinghe NP, Guggenheim S, de Dios AC, Ishii Y. J. Am. Chem. Soc. 2007; 129:10968. [PubMed: 17705472]
25. Meier BH, Storm CB, Earl WL. J. Am. Chem. Soc. 1986; 108:6072. [PubMed: 22175392]
26. Bertini, I.; Luchinat, C.; Parigi, G. Solution NMR of paramagnetic molecules. Elsevier Science B. V.; Amsterdam, The Netherlands: 2001.
27. Nayeem A, Yesinowski JP. J. Chem. Phys. 1988; 89:4600.
28. Wickramasinghe NP, Shaibat M, Ishii Y. J. Phys. Chem. B. 2007; 111:9693. [PubMed: 17661508]
29. Bovill AJ, McConnell AA, Nimmo JA, Smith WE. J. Phys. Chem. 1986; 90:569.
30. Basova TV, Kolesov BA. J. Struct. Chem. 2000; 41:770.
31. Abragam, A. Principles of nuclear magnetism. Oxford University Press; New York: 1961.
32. Solomon I. Phys. Rev. 1955; 99:559.
33. Zhang Y, Sun HH, Oldfield E. J. Am. Chem. Soc. 2005; 127:3652. [PubMed: 15771472]
34. Kobayashi N, Mack J, Ishii K, Stillman M. J. Inorg. Chem. 2002; 41:5350.
35. Zhang XX, Kobayashi N, Jiang JZ. Spectrochimi. Acta, Part A. 2006; 64:526.
36. Schmidt-Rohr, K.; Spiess, HW. Multidimensional solid-state NMR and polymers. Academic Press Inc.; San Diego: 1994.
37. Aroca R, Dilella DP, Loutfy RO. J. Phys. Chem. Solids. 1982; 43:707.
38. Ding HM, Wang S, Xi SQ. J. Mol. Struct. 1999; 475:175.
39. Tackley DR, Dent G, Smith WE. Phys. Chem. Chem. Phys. 2001; 3:1419.
40. Abe M, Kitagawa T, Kyogoku Y. J. Chem. Phys. 1978; 69:4526.
41. Lomax SQ. J. Coat. Technol. Res. In press.
42. Chen Q, Hou SS, Schmidt-Rohr K. Solid State Nucl. Magn. Reson. 2004; 26:11. [PubMed: 15157534]
43. Mao JH, Zhang Y, Oldfield E. J. Am. Chem. Soc. 2002; 124:13911. [PubMed: 12431123]
44. Greiner SP, Rowlands DL, Kreilick RW. 1992; 96:9132.

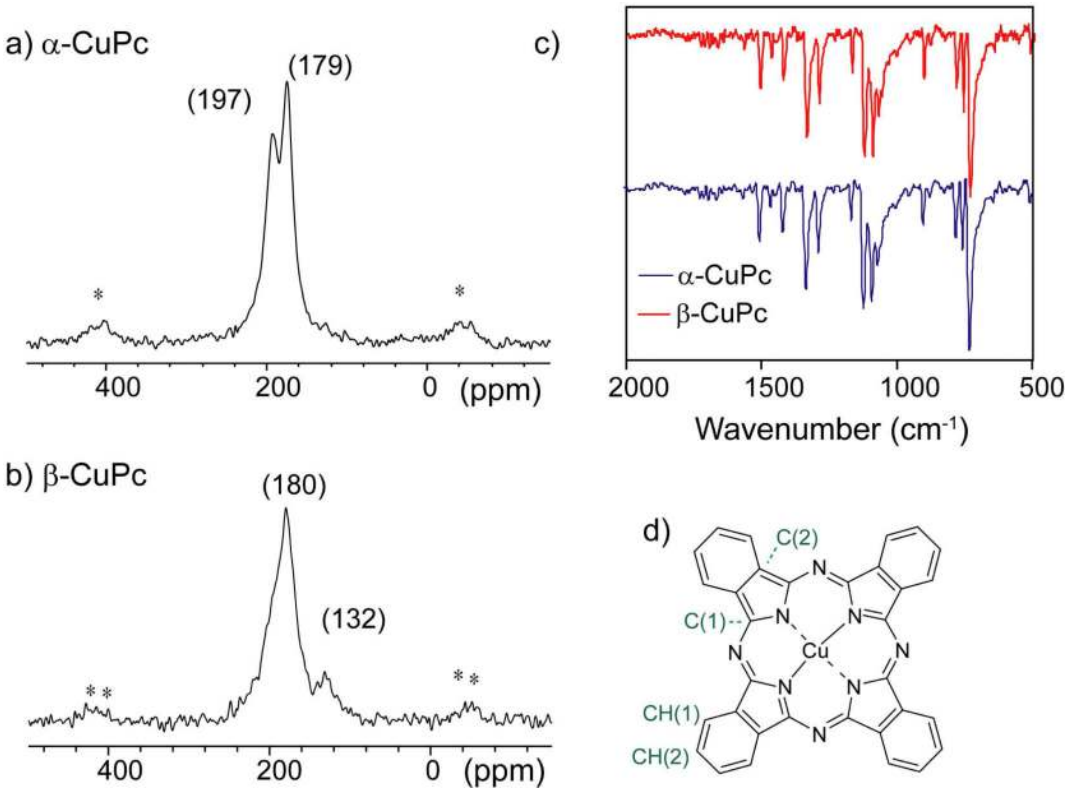

Figure 1.

^{13}C SSNMR MAS spectra of (a) α-CuPc (19.1 mg) and (b) β-CuPc (12.9 mg) obtained at ^{13}C frequency of 100.657 MHz without decoupling and with a single π/2-pulse excitation and a rotor synchronous echo sequence. The spectra were acquired at spinning speed of 22.989 kHz ± 5 Hz and −10 °C for the CuPc samples. The pulse delays were 120 ms and 50 ms for (a) and (b), respectively. The experimental time for the samples was 3.0 h for 81920 scans (a) and 205.7 min 3.4 h for 204800 scans for (b). The same conditions were used to collect background spectra using the scheme in ref. [42] with the equal experimental time. The spectra in (a) and (b) display the difference. The spectra in both (a) and (b) were processed with Gaussian broadening of 300 Hz. The peaks labeled by * in (a, b) denote spinning side bands. The signal-to-noise ratio for the tallest peaks at (a) 179 ppm and (b) 180 ppm are 41.8 and 28.2, respectively. (c) IR spectra of α-CuPc (blue, bottom) and β-CuPc (red, top) obtained with 256 scans. (d) A molecular structure of CuPc.

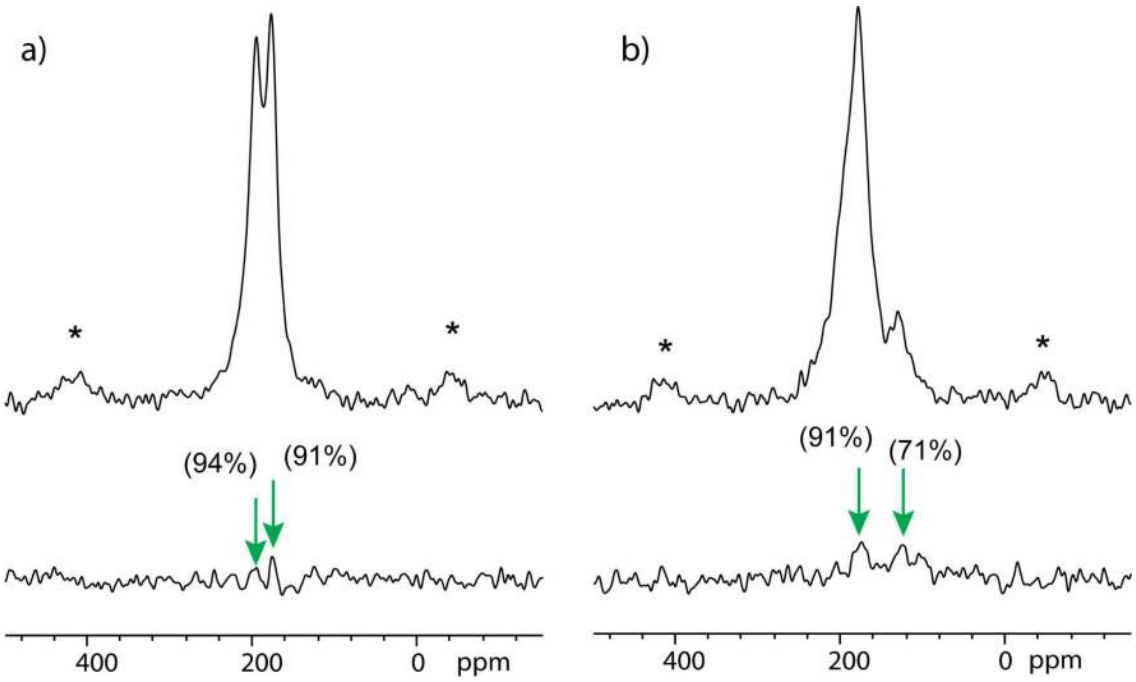

Figure 2.

^{13}C MAS spectra of (a) α-CuPc and (b) β-CuPc without (top) and with (bottom) ^{13}C-^{1}H REDOR dipolar dephasing. The spectra were obtained at 100.657 MHz without decoupling and with a single π/2-pulse excitation and a rotor synchronous echo sequence. The spectra were acquired at spinning speed of 22,989 Hz ± 5 Hz and −10 °C for the CuPc samples. ^{1}H and ^{13}C π-pulse widths are 5 μs, and the pulse delays were 50 ms. The experimental time for the α-CuPc sample (19.1 mg) was 1.4 h (81,920 scans) for the top or bottom spectrum in (a) while that for the β-CuPc sample (12.9 mg) was 3.4 h (204,800 scans) for the top or bottom spectrum in (b). The same conditions were used to collect corresponding background spectra using the scheme in ref. [42] with the equal experimental time. The spectra in (a) and (b) show difference spectra. Other parameters of the ^{13}C-^{1}H REDOR sequence are the same as those in ref. [17]. Refer to ref. [17] about the pulse sequence and other details. The spectra were processed with Gaussian broadening of 500 Hz.

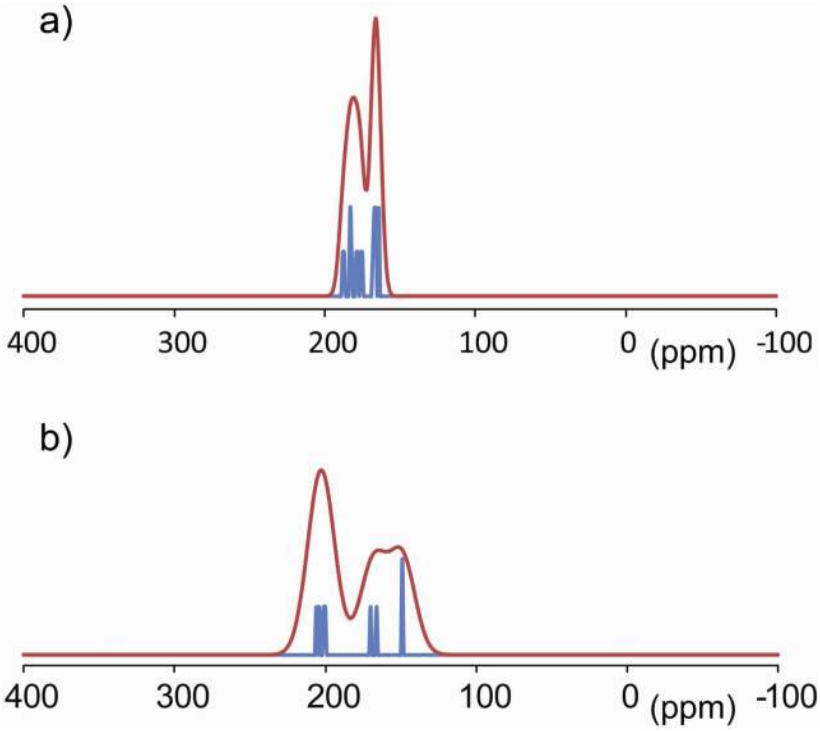

Figure 3.

Simulated ^{13}C spectra for ^{13}CH groups of (a) α-CuPc and (b) β-CuPc obtained from *ab initio* calculations of ^{13}C chemical shift (blue) without broadening and (red) with Gaussian broadening of (a) 7 ppm and (b) 20 ppm in the full width at the half height. The ratio of the line broadening widths is approximately matched to that for ^{13}C $1/T_1$ values observed for α- and β-CuPc. See Tables 2 and 3 for the calculated shift positions.

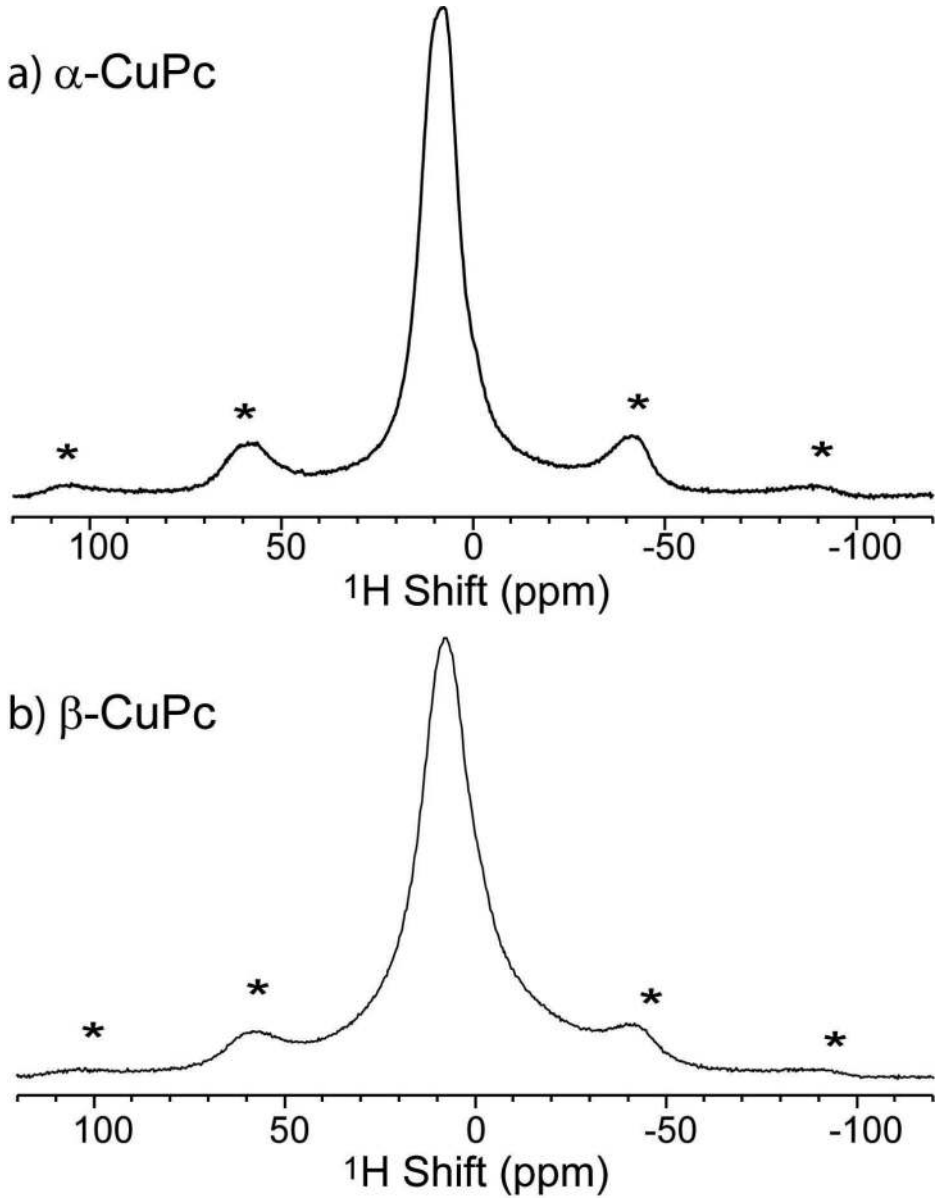

Figure 4.

^{1}H SSNMR spectra of (a) α-CuPc (19.1 mg) and (b) β-CuPc (12.5 mg) obtained at an NMR frequency of 400.214 MHz and a spinning speed of 20 kHz ± 5.0 Hz with a VT air set −10 °C. The spectra were obtained with (a) 32 scans and (b) 512 scans with pulse delays of 0.1 sec. Both spectra were obtained without applying any line broadening. (Spinning side bands are denoted with *).

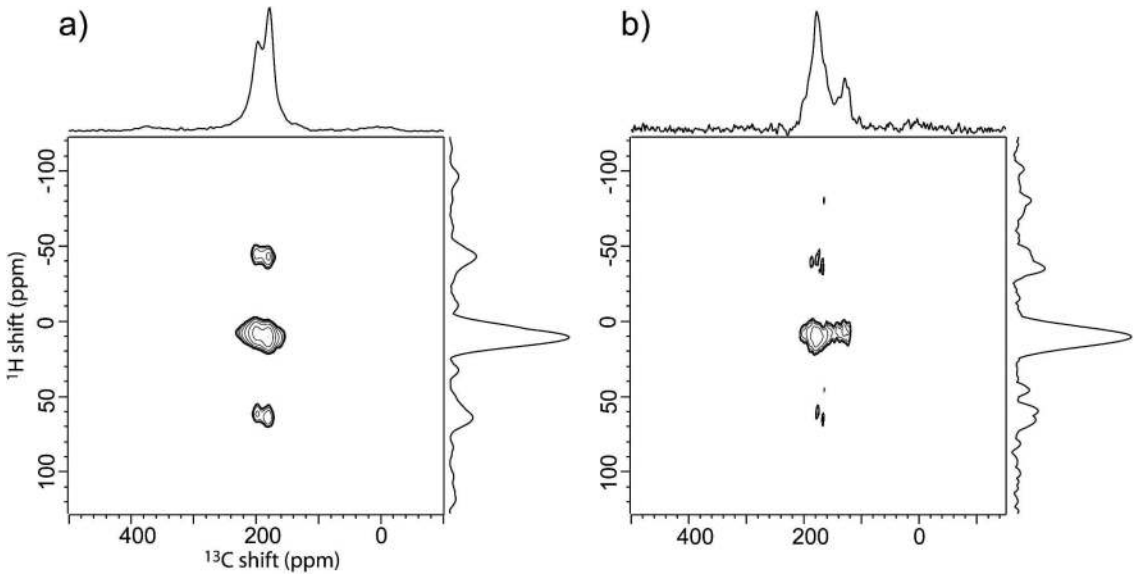

Figure 5.

2D ^{13}C/^{1}H correlation SSNMR spectra of (a) α-CuPc and (b) β-CuPc obtained with dipolar INEPT sequence[19] with τ = 5.0 μs at −10 °C and 20,000 ± 5.0 Hz spinning speed. For both ^{1}H and ^{13}C spins, $\pi/2$- and π-pulse width were 2.5 and 5.0 μs, respectively. 15 t_1 complex points were recorded with 46,080 scans for each t_1 real/imaginary point using a t_1 increment of 10.0 μs ($\tau_R/2$). The pulse delay was 50 ms and the experimental time was 20 h. Gaussian broadening was applied for both dimensions, with line widths of 500 Hz for (a) and (b).

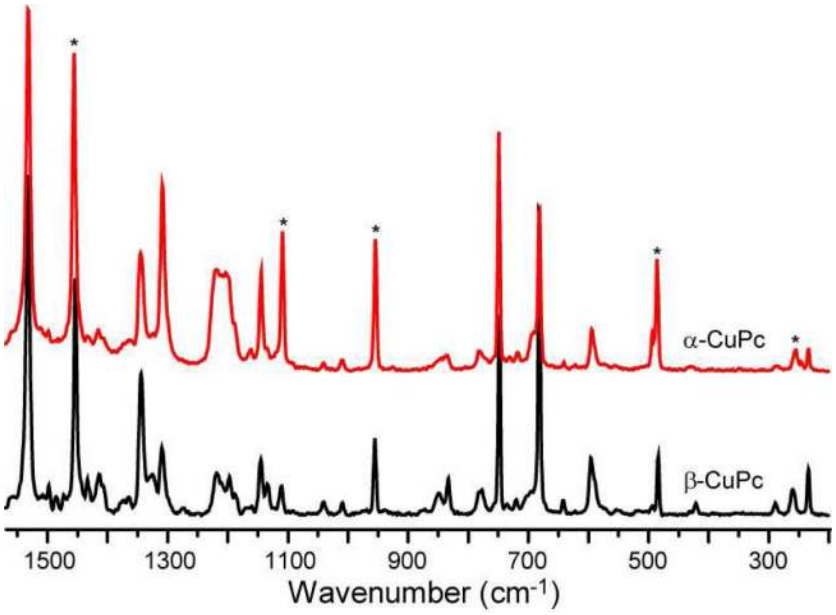

Figure 6.
Raman spectra of α-CuPc and β-CuPc. Spectra were collected for 60 seconds in extended scan mode between 3300 and 200 cm^{-1}. A total of ten accumulations were added to provide the presented data. Peaks denoted with stars exhibit shifts diagnostic for polymorphism.

Table 1

^{13}C T_1 relaxation times for α- and β-forms of CuPc.

Crystal form	**^{13}C T_1 relaxation time**		
α-CuPc	Peak position	179 ppm	197 ppm
	^{13}C T_1	38.3 ± 2.1 ms	25.1 ± 2.1 ms
β-CuPc	Peak position	132 ppm	180 ppm
	^{13}C T_1	14.0 ± 2.3 ms	8.6 ± 0.4 ms

Table 2

Calculated carbon chemical shifts for α-CuPc

Calculated shielding or shift for α-CuPc				
Carbon	**Diamagnetic Shielding**	**Diamagnetic Shift**	**Hyperfine Shift**	**Chemical Shift**
C(1)	22.0	163.0	572.5	735.5
	26.4	158.6	647.0	805.7
	24.3	160.7	664.8	825.5
	21.3	163.7	664.8	828.5
	21.9	163.1	604.5	767.5
	26.5	158.5	714.5	873.0
	24.5	160.5	735.8	896.3
	21.4	163.6	670.7	834.3
C(2)	43.3	141.7	598.5	740.2
	50.6	134.4	561.9	696.3
	49.0	136.0	563.1	699.1
	45.7	139.3	591.4	730.8
	43.3	141.7	602.1	743.8
	50.6	134.4	532.3	666.7
	49.0	136.0	525.2	661.2
	45.7	139.3	606.8	746.1
CH(1)	58.4	126.6	55.6	182.2
	61.7	123.3	40.2	163.5
	64.1	120.9	44.9	165.8
	63.7	121.3	61.5	182.8
	58.4	126.6	52.0	178.7
	61.7	123.3	52.0	175.3
	64.1	120.9	66.2	187.1
	63.7	121.3	44.9	166.2
CH(2)	52.4	132.6	34.3	166.9
	55.8	129.2	48.5	177.6
	56.5	128.5	54.4	182.9
	54.6	130.4	37.9	168.2
	52.4	132.6	43.8	176.3
	55.8	129.2	37.9	167.0
	56.5	128.5	35.5	164.0
	54.6	130.4	58.0	188.3

Table 3

Calculated carbon chemical shifts for β-CuPc

Calculated shielding or shift for β-CuPc (ppm)				
Carbon	**Diamagnetic Shielding**	**Diamagnetic Shift**	**Hyperfine Shift**	**Chemical Shift**
C(1)	30.1	154.9	590.3	745.1
	30.1	154.9	684.9	839.8
	32.3	152.7	696.7	849.4
	30.3	154.7	493.3	648.0
	30.1	154.9	590.3	745.1
	30.1	154.9	684.9	839.8
	32.3	152.7	696.7	849.4
	30.3	154.7	493.3	648.0
C(2)	46.7	138.3	635.2	773.5
	49.6	135.4	542.9	678.3
	50.2	134.8	537.0	671.9
	44.4	140.6	630.5	771.1
	46.7	138.3	635.2	773.5
	49.6	135.4	542.9	678.3
	50.2	134.8	537.0	671.9
	44.4	140.6	630.5	771.1
CH(1)	62.5	122.5	43.8	166.3
	63.1	121.9	79.3	201.1
	63.9	121.1	85.2	206.3
	61.2	123.8	46.1	169.9
	62.5	122.5	43.8	166.3
	63.1	121.9	79.3	201.1
	63.9	121.1	85.2	206.3
	61.2	123.8	46.1	169.9
CH(2)	54.8	130.2	69.8	200.0
	57.2	127.8	21.3	149.1
	56.3	128.7	20.1	148.8
	52.9	132.1	72.2	204.2
	54.8	130.2	69.8	200.0
	57.2	127.8	21.3	149.1
	56.3	128.7	20.1	148.8
	52.9	132.1	72.2	204.2

Table 4

Raman bands and shifts observed for α- and β-CuPc.

Assignment *a)*	α-CuPc (cm^{-1})	β-CuPc (cm^{-1})	Shift (cm^{-1})	Vibration Type *b)*
ν_{28}	1455.68	1453.77	−1.91	Macroring stretching
ν_{14}	1109.07	1111.26	2.19	C-H deformation
ν_{31}	954.33	955.33	1.00	Isoindole deformation
ν_{25}	485.82	484.14	−1.68	Isoindole deformation
ν_{52}	255.91	259.98	4.07	Cu–M deformation

*a)*The assignments are based on reference 29.

*b)*For the definitions of the vibration types, see references30,38,40.